Robotica (2004) volume 22, pp. 369–374. © 2004 Cambridge University Press
DOI: 10.1017/S0263574704000335 Printed in the United Kingdom

# Autonomous navigation of indoor mobile robots using a global ultrasonic system

Soo-Yeong Yi* and Byoung-Wook Choi**

(Received in Final Form: January 31, 2004)

**SUMMARY**

Autonomous navigation of an indoor mobile robot, using the global ultrasonic system, is presented in this paper. Since the trajectory error of the dead-reckoning navigation increases significantly with time and distance, the autonomous navigation system of a mobile robot requires self-localization capability in order to compensate for trajectory error. The global ultrasonic system, consisting of four ultrasonic generators fixed at *a priori* known positions in the work space and two receivers mounted on the mobile robot, has a similar structure to the well-known satellite GPS(Global Positioning System), which is used for the localization of ground vehicles. The EKF (Extended Kalman Filter) algorithm is utilized for self-localization and autonomous navigation, based on the self-localization algorithm is verified by experiments performed in this study. Since the self-localization algorithm is efficient and fast, it is appropriate for an embedded controller of a mobile robot.

KEYWORDS: Autonomous navigation; Self-localization; Global ultrasonic system; Radio frequency module; Extended kalman filter.

## 1. INTRODUCTION

For autonomous navigation in the work space, the mobile robot needs to have a self-localization capability and motion control functions required to figure out where it is and in which direction it should move[1]. Since the trajectory error of a dead-reckoning navigation system, which relies only on the internal sensor such as the odometer or the encoder, grows with time and distance, an external sensor such as a camera vision or ultrasonic sensors is necessary in order to localize the position of the robot in the work space and to compensate for the trajectory error. The possible methods of self-localization using external sensors can be divided into two groups: local methods and global methods. In the local method, a mobile robot makes a local object map using the relative distance data from the environmental objects and matches the local map with a global map database. As a result, the mobile robot figures out its own position in the work-space. On the other hand, in the global method, the mobile robot computes its position directly in the global coordinates using the distances from some reference positions in the work space.

The local method has some advantages in that collision-avoidance motion and map-reconstruction for the transformed environment are made possible by using the distance sensors on the robot, as well as the self-localization system. However, this requires massive computations in terms of the local map-making and the matching processes with the global map database. In the extreme case, the robot has to stop moving momentarily, in order to obtain the necessary environmental information[2,3]. On the other hand, in the global method, the local map-making and the matching processes are avoidable, and the self-localization is computationally efficient and fast[4,5]. The global localization method is exemplified by the well-known satellite GPS system, in which the localization process is based on triangulation using the distances between the GPS receiver on a mobile object and three or more signal transmitters, i.e. satellites in the earth coordinates[6]. Although the GPS system has received increasing attention in recent years, obtaining a sufficient level of positioning accuracy is still quite expensive. Moreover, it is difficult to use GPS for indoor applications due to the shielding effect.

The global ultrasonic system presented in this paper is a kind of an active ultrasonic system[7], having a GPS like structure for the self-localization of an indoor mobile robot. The ultrasonic sensor is regarded as the most cost-effective ranging system among the possible alternatives, and it is widely used for general purposes, since it requires simple electronic drivers and has relatively high accuracy[8]. The global ultrasonic system consists of four or more ultrasonic generators fixed at reference positions in the global coordinates and two receivers mounted on the mobile robot. By using the RF (Radio Frequency) modules added to the ultrasonic sensors, the robot is able to control the ultrasonic generation and to obtain the critical distances from the reference positions, which are required in order to localize its position in the global coordinates. In this paper, we propose a kalman filter algorithm designed for self-localization using the global ultrasonic system, while verifying the performance of the autonomous navigation system based on the self-localization through various experiments.

* Division of Electronics and Information Engineering, Chonbuk National University (South Korea) (Tel: +82-63-270-4283; E-mail: suylee@moak.chonbuk.ac.kr)
** Department of Control and Measurement Engineering, Sunmoon University (South Korea) (Tel: +82-41-530-2349; E-mail: bwchoi@sunmoon.ac.kr)

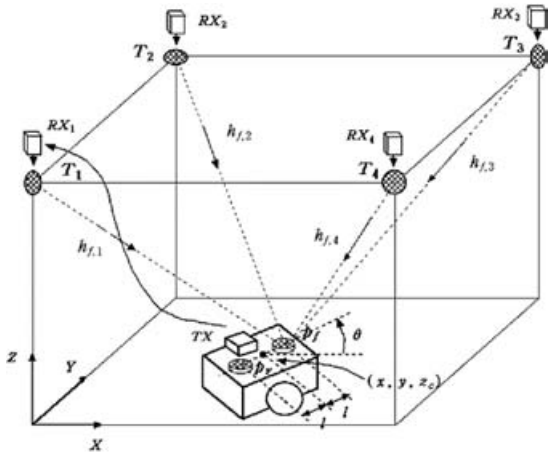


Fig. 1. The global ultrasonic system.

## 2. THE GLOBAL ULTRASONIC SYSTEM

The overall structure of the global ultrasonic system is depicted in Fig. 1. The ultrasonic generators are fixed at known positions, $\boldsymbol{T}_i = [x_i, y_i, z_i]^t$, $i = 1, \ldots, 4$ in the work space, e.g. at each corner of the ceiling. Using the front and the rear ultrasonic sensors situated at $\boldsymbol{P}_f$ and $\boldsymbol{P}_r$, the mobile robot receives the ultrasonic signal and computes the distances by counting the TOF (Time Of Flight) of the signal. It is conveniently assumed in Fig. 1 that the number of ultrasonic generators is four, which can be increased as needed in consideration of the work-space size and the objects in the immediate environment. In order to avoid cross-talk between the ultrasonic signals and to synchronize the ultrasonic receivers with the generators, the RF receivers, $RX_1 \sim RX_4$, and the RF transmitter, $TX$, are added to the ultrasonic generators and the ultrasonic receivers on the robot, respectively. By using the RF channel, the mobile robot sequentially activates each one of the ultrasonic generators in successive time slots. Assuming that the delivery time for the RF calling signal is negligible, the ultrasonic signal generation occurs simultaneously with the RF calling signal transmission and it is possible to synchronize the ultrasonic generators and the receivers. In Fig. 1, $h_{f,1} \sim h_{f,4}$ denote the distance between $\boldsymbol{T}_1 \sim \boldsymbol{T}_4$ and $\boldsymbol{P}_f$. The distances, $h_{r,1} \sim h_{r,4}$, between $\boldsymbol{T}_1 \sim \boldsymbol{T}_4$ and $\boldsymbol{P}_r$ are omitted for brevity. The positions of the ultrasonic receivers on the robot, $\boldsymbol{P}_f = [x_f, y_f, z_c]^t$ and $\boldsymbol{P}_r = [x_r, y_r, z_c]^t$, with respect to the center position of the mobile robot, $\boldsymbol{P} = [x, y, z_c]^t$, can be described as follows:

$$\boldsymbol{P}_f = \begin{bmatrix} x + l\cos\theta \\ y + l\sin\theta \\ z_c \end{bmatrix}, \quad \boldsymbol{P}_r = \begin{bmatrix} x - l\cos\theta \\ y - l\sin\theta \\ z_c \end{bmatrix} \tag{1}$$

where $l$ represents the distance between the center position of the mobile robot and the ultrasonic receiver, and $\theta$ denotes the heading angle of the mobile robot. It is assumed that the moving surface is flat, so that the $z$ component of the position vectors is constant as $z_c$ in (1).

## 3. THE EKF FOR THE SELF-LOCALIZATION AND THE AUTONOMOUS NAVIGATION ALGORITHM

The position vector in the $x - y$ plane, $\boldsymbol{r} = [x, y]^t$, together with the heading angle, $\theta$, of a mobile robot having differential wheels, follows the state equation (2) in the discrete-time domain[9]:

$$\begin{bmatrix} x_{k+1} \\ y_{k+1} \end{bmatrix} = \begin{cases} \begin{bmatrix} x_k + T\upsilon_k\cos\theta_k \\ y_k + T\upsilon_k\sin\theta_k \end{bmatrix} & if\ \omega_k = 0 \\ \begin{bmatrix} x_k + \rho_k\cos\theta_k\sin(T\omega_k) \\ \quad - \rho_k\sin\theta_k(1 - \cos(T\omega_k)) \\ x_k + \rho_k\cos\theta_k\sin(T\omega_k) \\ \quad + \rho_k\sin\theta_k(1 - \cos(T\omega_k)) \end{bmatrix} & if\ \omega_k \neq 0 \end{cases}$$

$$\theta_{k+1} = \theta_k + T\omega_k \tag{2}$$

where the subscript $k$ is the time index, $T$ denotes the sampling interval, $\upsilon_k$ and $\omega_k$ are the linear and the angular velocities of the robot, respectively, and $\rho_k = \frac{\upsilon_k}{\omega_k}$ represents the radius of rotation. The position vector and the heading angle of the mobile robot are augmented so as to become $\boldsymbol{p} = [x, y, \theta]^t$, which is referred to as the robot posture. The bold and normal symbols represent the vector and the scalar variables, respectively.

As a consequence of (1) and (2), the state equation for the ultrasonic receivers on the robot can be described as follows:

$$\boldsymbol{r}_{f,k+1} = \boldsymbol{f}_f(r_{f,k}, \boldsymbol{u}_k, \boldsymbol{q}_k)$$

$$= \begin{cases} \begin{bmatrix} x_{f,k} + T\upsilon_k\cos\theta_k + q_{1,k} \\ y_{f,k} + T\upsilon_k\sin\theta_k + q_{2,k} \end{bmatrix} & if\ \omega_k = 0 \\ \begin{bmatrix} x_{f,k} - (l\cos\theta_k + \rho_k\sin\theta_k)(1 - \cos(T\omega_k)) \\ \quad + (-l\sin\theta_k + \rho_k\cos\theta_k)\sin(T\omega_k) + q_{1,k} \\ y_{f,k} + (-l\sin\theta_k + \rho_k\cos\theta_k)(1 - \cos(T\omega_k)) \\ \quad + (l\cos\theta_k + \rho_k\sin\theta_k)\sin(T\omega_k) + q_{2,k} \end{bmatrix} & if\ \omega_k \neq 0 \end{cases} \tag{3-1}$$

$$\boldsymbol{r}_{r,k+1} = \boldsymbol{f}_r(\boldsymbol{r}_{r,k}, \boldsymbol{u}_k, \boldsymbol{q}_k)$$

$$= \begin{cases} \begin{bmatrix} x_{r,k} + T\upsilon_k\cos\theta_k + q_{1,k} \\ y_{r,k} + T\upsilon_k\sin\theta_k + q_{2,k} \end{bmatrix} & if\ \omega_k = 0 \\ \begin{bmatrix} x_{r,k} - (l\cos\theta_k + \rho_k\sin\theta_k)(1 - \cos(T\omega_k)) \\ \quad + (-l\sin\theta_k + \rho_k\cos\theta_k)\sin(T\omega_k) + q_{1,k} \\ y_{r,k} + (-l\sin\theta_k + \rho_k\cos\theta_k)(1 - \cos(T\omega_k)) \\ \quad + (l\cos\theta_k + \rho_k\sin\theta_k)\sin(T\omega_k) + q_{2,k} \end{bmatrix} & if\ \omega_k \neq 0 \end{cases} \tag{3-2}$$

where $\boldsymbol{r}_f = [x_f, y_f]^t$ and $\boldsymbol{r}_r = [x_r, y_r]^t$ represent the positions of the front and rear ultrasonic receivers, respectively, and $\boldsymbol{q}_k = [q_{1,k}, q_{2,k}]^t$ is the Gaussian random noise with zero mean and $\boldsymbol{Q}$ variance. The measurement equation at the ultrasonic receivers can be modeled as follows:

$$z_{f,k} = h_{f,i}(r_{f,k}, v_k)$$
$$= \{(x_{f,k} - x_i)^2 + (y_{f,k} - y_i)^2 + (z_c - z_i)^2\}^{1/2} + v_k \tag{4-1}$$

$$z_{r,k} = h_{r,i}(r_{r,k}, v_k)$$
$$= \{(x_{r,k} - x_i)^2 + (y_{r,k} - y_i)^2 + (z_c - z_i)^2\}^{1/2} + v_k \tag{4-2}$$

https://doi.org/10.1017/S0263574704000335 Published online by Cambridge University Press

where the measurement noise, $\upsilon_k$, is assumed to be Gaussian with zero mean and $G$ variance, and the subscript, $i$, denotes one of the ultrasonic generators, $\boldsymbol{T}_1 \sim \boldsymbol{T}_4$, which is called by the mobile robot at time $k$.

From the state Eq. (3-1) and the measurement Eq. (4-1), it is possible to get the following set of equations constituting the EKF estimation for the front ultrasonic receiver position:

$$\begin{aligned} \hat{\boldsymbol{r}}^-_{f,k+1} &= \boldsymbol{f}_f(\hat{\boldsymbol{r}}_{f,k}, \boldsymbol{u}_k, \boldsymbol{0}) \\ \boldsymbol{V}^-_{f,k+1} &= \boldsymbol{A}_{f,k}\boldsymbol{V}_{f,k}\boldsymbol{A}^t_{f,k} + \boldsymbol{Q} \end{aligned} \tag{5}$$

$$\begin{aligned} \boldsymbol{K}_{f,k} &= \boldsymbol{V}^-_{f,k}\boldsymbol{H}^t_{f,k}\left(\boldsymbol{H}_{f,k}\boldsymbol{V}^-_{f,k}\boldsymbol{H}^t_{f,k} + G\right)^{-1} \\ \boldsymbol{V}_{f,k} &= (\boldsymbol{I} - \boldsymbol{K}_{f,k}\boldsymbol{H}_{f,k})\boldsymbol{V}^-_{f,k} \\ \hat{\boldsymbol{r}}_{f,k} &= \hat{\boldsymbol{r}}^-_{f,k} + \boldsymbol{K}_{f,k}(z_{f,k} - h_{f,i}(\hat{\boldsymbol{r}}^-_{f,k}, \boldsymbol{0})) \end{aligned} \tag{6}$$

where $\boldsymbol{K}_{f,k}$ is the kalman filter gain, $\hat{\boldsymbol{r}}^-_{f,k}$ and $\hat{\boldsymbol{r}}_{f,k}$ represents the *a priori* and *a posteriori* estimations for $\boldsymbol{r}_{f,k}$, respectively, and $\boldsymbol{V}^-_{f,k}$ and $\boldsymbol{V}_{f,k}$ represent the *a priori* and *a posteriori* error covariance matrices, respectively, as defined in (7).

$$\begin{aligned} \boldsymbol{V}^-_{f,k} &= \boldsymbol{E}[(\boldsymbol{r}_{f,k} - \hat{\boldsymbol{r}}^-_{f,k})(\boldsymbol{r}_{f,k} - \hat{\boldsymbol{r}}^-_{f,k})^t] \\ \boldsymbol{V}_{f,k} &= \boldsymbol{E}[(\boldsymbol{r}_{f,k} - \hat{\boldsymbol{r}}_{f,k})(\boldsymbol{r}_{f,k} - \hat{\boldsymbol{r}}_{f,k})^t] \end{aligned} \tag{7}$$

where $\boldsymbol{E}(\cdot)$ denotes the expectation of the corresponding random variables. The Jacobian matrices, $\boldsymbol{A}_{f,k}$ and $\boldsymbol{H}_{f,k}$, in (6) are given as follows:

$$\begin{aligned} \boldsymbol{A}_{f,k} &= \frac{\partial \boldsymbol{f}_f}{\partial \boldsymbol{r}_{f,k}}(\hat{\boldsymbol{r}}_{f,k}, \boldsymbol{u}_k, \boldsymbol{0}) \\ &= \begin{bmatrix} 1 & 0 \\ 0 & 1 \end{bmatrix} \end{aligned} \tag{8}$$

$$\begin{aligned} \boldsymbol{H}_{f,k} &= \frac{\partial h_{f,i}}{\partial \boldsymbol{r}_{f,k}}(\hat{\boldsymbol{r}}_{f,k}, \boldsymbol{0}) \\ &= \begin{bmatrix} \dfrac{x_{f,k} - x_i}{D_{f,i}} & \dfrac{y_{f,k} - y_i}{D_{f,i}} \end{bmatrix} \end{aligned} \tag{9}$$

where $D_{f,i}$ is defined by the following Eq. (10).

$$D_{f,i} = \{(x_{f,k} - x_i)^2 + (y_{f,k} - y_i)^2 + (z_c - z_i)^2\}^{1/2} \tag{10}$$

The EKF estimation, $\hat{\boldsymbol{r}}_{r,k}$, for the rear ultrasonic receiver position is similar and omitted here for the sake of brevity.

From $\hat{\boldsymbol{r}}_{f,k}$ and $\hat{\boldsymbol{r}}_{r,k}$, the posture estimation for the mobile robot can be described as follows:

$$\begin{aligned} \hat{x}_k &= \frac{\hat{x}_{f,k} + \hat{x}_{r,k}}{2} \\ \hat{y}_k &= \frac{\hat{y}_{f,k} + \hat{y}_{r,k}}{2} \\ \hat{\theta}_k &= \tan^{-1}\frac{\hat{y}_{f,k} - \hat{y}_{r,k}}{\hat{x}_{f,k} - \hat{x}_{r,k}} \end{aligned} \tag{11}$$

Assuming that the estimation error covariances for the front and the rear ultrasonic receiver positions are the same, the error covariances of the posture estimation are given in (12) as shown in Fig. 2.

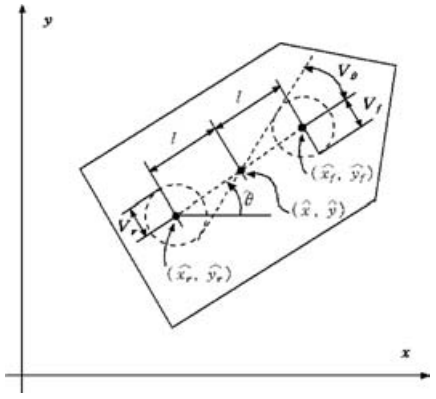


Fig. 2. Error covariances of the posture estimation.

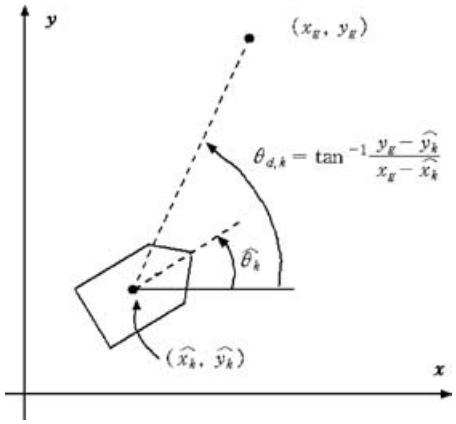


Fig. 3. Navigation control.

$$\begin{aligned} \boldsymbol{V}_{p,k} &= \boldsymbol{E}[(\boldsymbol{r} - \hat{\boldsymbol{r}}_k)(\boldsymbol{r} - \hat{\boldsymbol{r}}_k)^2] \\ &= \boldsymbol{V}_{f,k}(= \boldsymbol{V}_{r,k}) \\ \boldsymbol{V}_{\theta,k} &= \boldsymbol{E}[(\theta - \theta_k)^2] \\ &\approx \tan^{-1}\frac{\boldsymbol{V}_{f,k}}{l} \end{aligned} \tag{12}$$

Eq. (12) implies that the estimation for the heading angle becomes more accurate according to the distance between the two ultrasonic receivers. Based on the self-localization given in (11), a simple control input, $\upsilon_k$ and $\omega_k$, to drive the mobile robot toward the given goal position, $\boldsymbol{r_g} = [x_g, y_g]^t$ can be written as (13).

$$\begin{aligned} \upsilon_k &= c \\ \omega_k &= k_\theta(\theta_{d,k} - \theta_k), \quad \theta_{d,k} = \tan^{-1}\frac{y_g - \hat{y}_k}{x_g - \hat{x}_k} \end{aligned} \tag{13}$$

where $c$ and $k_\theta$ are positive constants. The mobile robot adjusts its heading angle toward the intended position and moves with the constant velocity, as depicted in Fig. 3.

## 4. EXPERIMENTS AND DISCUSSIONS

In order to verify the performance of the EKF self-localization and autonomous navigation system using the global

https://doi.org/10.1017/S0263574704000335 Published online by Cambridge University Press

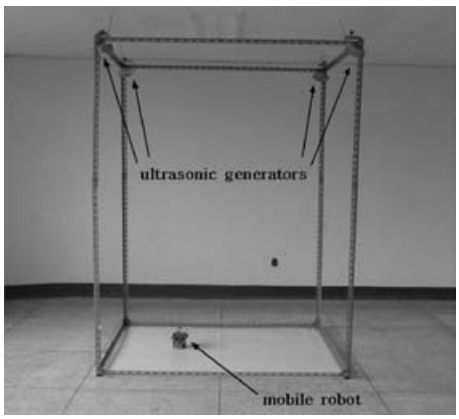


Fig. 4. Experimental setup.

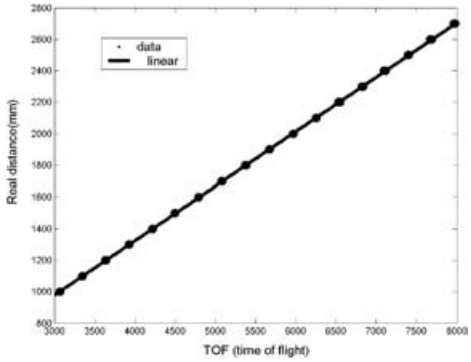


Fig. 5. Real distance with respect to ultrasonic TOF.

ultrasonic system, a simple experimental set-up was established, as shown in Fig. 4, which has dimension of 1,500 mm and 1,500 mm in width and length, respectively, and 2,500 mm in height. The ultrasonic generators installed with the RF receivers are fixed near the four corners of the ceiling, and whose positions are described in (14).

$$\begin{aligned} \boldsymbol{T}_1 &= [10.0, 10.0, 2360.0]^t \\ \boldsymbol{T}_2 &= [1427.0, 5.0, 2370.0]^t \\ \boldsymbol{T}_3 &= [1423.0, 1445.0, 2357.0]^t \\ \boldsymbol{T}_4 &= [0.0, 1380.0, 2370.0]^t \end{aligned} \tag{14}$$

At first, a preliminary experiment was carried out for the ultrasonic calibration and the result is presented in Fig. 5.

The linear equation relating the ultrasonic TOF to the real distance is given in (15), as obtained from the least-square method, and the variance of the measurement noise is specified as (16).

$$D = 0.34533 \cdot T - 57.224 \tag{15}$$

$$G = 1.8 \tag{16}$$

where $D$(mm) represents the real distance between the ultrasonic generator and the receiver, and $T(\mu\,\text{sec})$ is the ultrasonic TOF.

Fig. 6 shows the results of the self-localization experiment, in which the robot is moved manually from the initial posture,

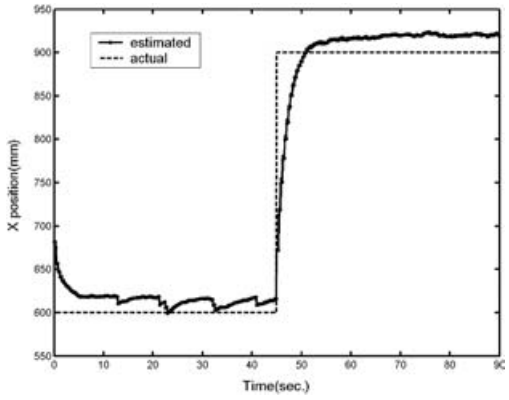


(a) Position estimation in $x$ axis

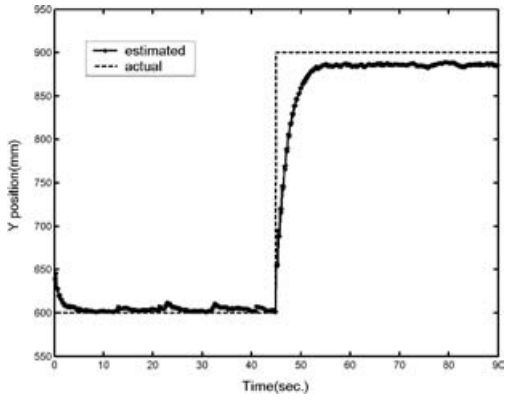


(b) Position estimation in $y$ axis

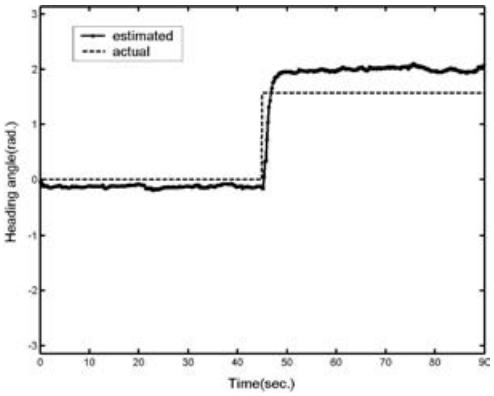


(c) Estimation for heading $\theta$ angle

Fig. 6. The self-localization of the mobile robot.

$(x, y, \theta) = (600, 600, 0)$ to the goal posture, $(900, 900, \pi/2)$ at 45 sec. The initial value of the posture estimation is set arbitrarily as (650, 650, 0). The distance and the heading angle are described by mm and rad., respectively. As shown in Fig. 6, the position errors in the $x$ and $y$ axes are less than 25 mm in the steady-state. Since the distance between the center position of the robot and the ultrasonic receiver is designed as $l = 75$ mm, the estimation error of the heading angle in (12) becomes $\tan^{-1}(25/75) \approx 0.32$ rad., as shown in Fig. 6(c).

The variances, $\boldsymbol{Q}$ and $G$, of the state noise and measurement noise in the EKF estimations, (3) and (4), represent the measure of the relative confidence. In the case of $\|\boldsymbol{Q}\| > G$ for example, the measurement data given in (4-1) and (4-2) obtained from the external sensors are more

https://doi.org/10.1017/S0263574704000335 Published online by Cambridge University Press

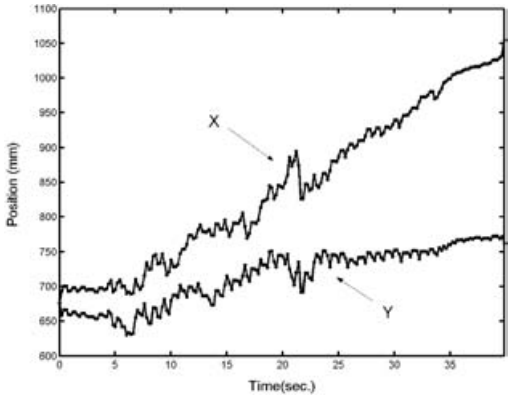


(a) Position in $x$ and $y$ axis

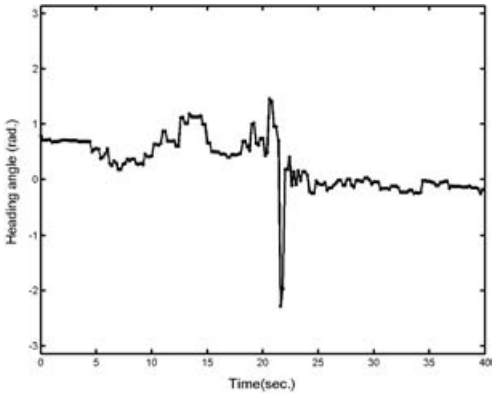


(b) Heading angle

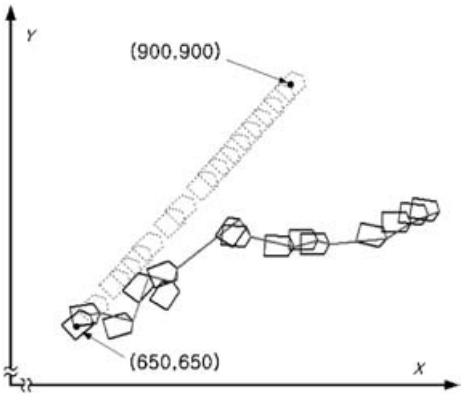


(c) Trajectory in $x - y$ plane

Fig. 7. The dead-reckoning navigation.

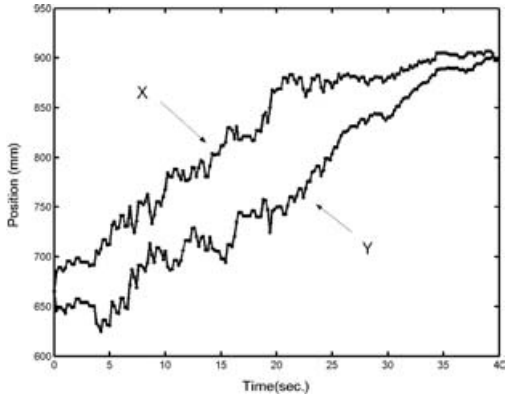


(a) Position in $x$ and $y$ axis

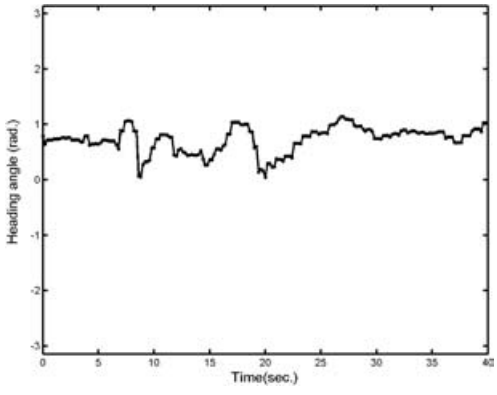


(b) Heading angle

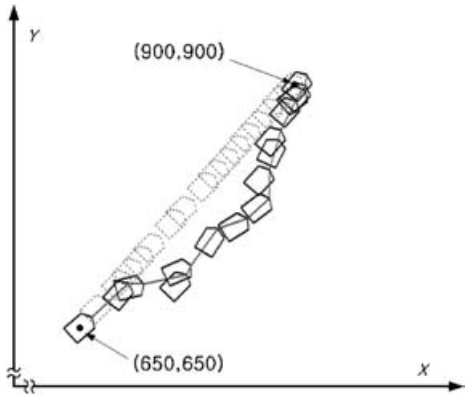


(c) Trajectory in $x - y$ plane

Fig. 8. Navigation with global ultrasonic system.

credible than the state value obtained from the motion determined by Eqs. (3-1) and (3-2). It is possible to obtain the variance of the measurement noise, $\boldsymbol{Q}$, by experiment, as described in (16). However, the variance of the state noise, $G$, is generally difficult to obtain, since it is caused by uncertainties, such as the slippage between the wheels and the ground or the unmodeled dynamics of the mobile robot. Thus, in this experiment, the variance of the state noise is intentionally set to $\boldsymbol{Q} = [50.0, 50.0]^t$, so as to give confidence to the measurement data obtained in the global ultrasonic system, rather than the state value obtained from (3).

The autonomous navigation system using the global ultrasonic system is compared to the dead-reckoning navigation system on the straight line connecting the initial posture, $(650, 650, \pi/4)$, and the goal posture, $(900, 900, \pi/4)$, in the work space. Fig. 7 shows the results in the case of the dead-reckoning navigation, in which the mobile robot cannot reach its goal posture, due to the uncertainties in the state equation. In Fig. 7(c), the dotted polygons represent the desired postures of the mobile robot with respect to time.

The results of the autonomous navigation system based on the self-localization using the global ultrasonic system are presented in Fig. 8 for the same initial and goal postures. As shown in this figure, the mobile robot reaches the goal posture, overcoming the uncertainties in the state equation, and the heading angle at the final position is around $\frac{\pi}{4}$, as desired. It should be noted that the posture data in Figs. 7 and 8 are obtained by using the global ultrasonic system also, thus these values may be different from the actual postures to some degree.

https://doi.org/10.1017/S0263574704000335 Published online by Cambridge University Press

The size of the ultrasonic region in the work space is dependant on the beam-width of the ultrasonic generator. In the case of a general ultrasonic ranging system, in which both the signal generator and the receiver are lumped together, an ultrasonic generator with a narrow beam-width is preferable in order to avoid the ambiguity and to enhance the measurement accuracy. On the other hand, the proposed global ultrasonic system, which has a distributed signal generator, requires the use of a wide beam-width generator, in order to expand the ultrasonic region in the work space.

## 5. CONCLUSIONS

In this paper, the global ultrasonic system with an EKF algorithm is presented for the self-localization of an indoor mobile robot. Also, the performance of the autonomous navigation based on the self-localization system is thus verified through various experiments. The global ultrasonic system consists of four or more ultrasonic generators fixed at known positions in the work space, two receivers mounted on the mobile robot, and RF modules added to the ultrasonic transducers. By controlling the ultrasonic signal generation through the RF channel, the robot can synchronize and measure the distance between the ultrasonic generators and receivers, thereby estimating its own position and heading angle. It is shown through experiment that the estimation errors are less than 25 mm in terms of the position and less than 0.32 rad. in terms of the heading angle. Since the estimation error of the heading angle is dependant on the distance between the two ultrasonic receivers on the robot, it is possible to obtain a more accurate estimation for the heading angle by increasing this distance.

The global ultrasonic system has the following salient features: (1) simple and efficient state estimation, since the process of local map-making and matching with the global map database is avoidable, due to the GPS-like nature of the system, (2) active cuing of the ultrasonic generation time and sequence through the RF channel, and (3) robustness against signal noise, since the ultrasonic receiver on the mobile robot processes the signal received directly from the generator, instead of through an indirect reflected signal.

In this paper, it is assumed an ideal environment exists without any objects in the work-space. Environmental objects may result in an area of relative obscurity, which the ultrasonic signals cannot reach. It is possible to overcome the problems associated with environments containing obstacles by increasing the number of ultrasonic generators in the work space as needed. This enhancement is currently being studied.

## References

1. S. Singh and P. Keller, "Obstacle detection for high speed autonomous navigation", *Proc. of IEEE Int. Conf. on Robotics and Automation* (1991) pp. 2798–2805.
2. J. Leonard and H. Durrant-Whyte, *Directed sonar sensing for mobile robot navigation*, Kluwer Academic Publishers (1992).
3. J. Ko, W. Kim and M. Chung, "A Method of Acoustic Landmark Extraction for Mobile Robot Navigation", *IEEE Trans. on Robotics and Automation* **12**(6), 478–485 (1996).
4. J. Leonard and H. Durrant-Whyte, "Mobile Robot Localization by Tracking Geometric Beacons", *IEEE Trans. on Robotics and Automation* **7**(3), 376–382 (1991).
5. S. Hernandez, J. M. Torres, C. A. Morales and L. Acosta, "A new low cost system for autonomous robot heading and position localization in a closed area", *Autonomous Robots* **15**, 99–110 (2003).
6. S. Haihang, G. Muhe and H. Kezhong, "An integrated GPS/CEPS position estimation system for outdoor mobile robot", *Proc. of IEEE Int'l Conf. on Intelligent Processing Systems* (1997) pp. 28–31.
7. L. Kleeman, "Optimal Estimation of Position and Heading for Mobile Robots Using Ultrasonic Beacons and Dead-reckoning", *Proc. of IEEE Conf. on Robotics and Automations* (1992) pp. 2582–2587.
8. R. Kuc and M. W. Siegel, "Physically based simulation model for acoustic sensor robot navigation". *IEEE Trans. on Pattern Anal. Machine Intell.* **9**(6), 766–777 (1987).
9. D. Fox, W. Burgard and S. Thrun, "The dynamic window approach to collision avoidance", *IEEE Robotics and Automation Magazine* 23–33, (March, 1997).

https://doi.org/10.1017/S0263574704000335 Published online by Cambridge University Press